ELSEVIER

Journal of Photochemistry and Photobiology A: Chemistry 154 (2003) 259–265

Journal of Photochemistry and Photobiology A:Chemistry

www.elsevier.com/locate/jphotochem

Infrared multiphoton dissociation of propynal: time resolved observation of CO ($\nu \geq 1$) IR emission at 4.7 μm

P.K. Chowdhury*

Radiation Chemistry and Chemical Dynamics Division, Bhabha Atomic Research Centre, Trombay, Mumbai 400 085, India

Received 3 April 2002; received in revised form 1 July 2002; accepted 30 August 2002

Abstract

In contrast to the electronically excited propynal at 193 nm undergoing aldehyde C–H and C–C bond ruptures, on pulsed TEA-CO_2 laser irradiation, multiphoton vibrationally excited propynal undergoes concerted dissociation generating CO and acetylene. Vibrational excitation in the CO product is detected immediately following the CO_2 laser pulse by observing infrared (IR) emission at 4.7 μm. The decay of the IR emission was studied as a function of propynal pressure. A vibrational–vibrational relaxation rate constant of CO ($\nu \geq 1$) by propynal is found to be $1540 \pm 200\ \text{Torr}^{-1}\ \text{s}^{-1}$. With the collisionless dissociation of propynal, the evaluated unimolecular rate constant of $(1.5 \pm 0.2) \times 10^7\ \text{s}^{-1}$, vis-a-vis RRKM calculations, gives an average IR multiphoton excitation level of propynal as $75 \pm 4\ \text{kcal mol}^{-1}$.

Keywords: Multiphoton dissociation; IR emission; Propynal

1. Introduction

The gas phase photochemistry of small aldehydes and ketones has been the subject of numerous investigations and has been reviewed recently by several authors [1–3]. Much effort has been devoted to the investigation of formaldehyde, the smallest member of the carbonyl series of compounds [3]. Excitation of the $S_1(n, \pi^*)$ state leads to the formation of H_2 and CO following a predissociation process [4]. However, at higher S_1 excitation energies above the threshold of 86 kcal/mol [5], a competing C–H bond fission channel opens up producing H and CHO radicals.

Propynal HC≡C–CHO is of particular interest because it is the smallest unsaturated carbonyl compound. As compared with formaldehyde, the aldehydic C–H bond fission energy has been determined by Willmott et al. [6] as 86.6 kcal/mol, indicating the absence of stabilization due to acetynyl group. In gas phase photolysis at 300–400 nm of propynal with the (n, π^*) S_1 or T_1 excitation, Stafast et al. [7] found the molecular photoproducts CO and C_2H_2, after internal conversion to the ground state. Whereas Haas et al. [8] reported three dissociation channels in the molecular beam photofragmentation of propynal at 193 nm, radical channel to form C_2H and HCO, hydrogen atom channel involving aldehyde C–H bond fission, as well as molecular channel to form CO and C_2H_2. By observing that most of the available energy is channeled into internal energy of the fragments and only a small amount in fragment translation, they suggested that the dissociation or bond rupture mechanism is via predissociation with a strong participation of the internal degrees of freedom.

To understand the dissociation mechanism under true vibrational excitation conditions, infrared multiphoton dissociation (IRMPD) of propynal from its ground electronic state has been studied. In contrast to the radical channels in the UV photochemistry, we report concerted molecular dissociation of propynal, when irradiated by a pulsed CO_2 laser, producing CO and C_2H_2 as primary products. As the concerted channel is near thermoneutral, a significant amount of vibrational excitation energy is expected to be associated with the primary products. IR emission of the hot fragment CO ($\nu \geq 1$) is monitored and also its collisional relaxation rate with the parent molecules is obtained.

2. Experimental

The experiments were performed with a static system at room temperature. The conventional setup which includes a photolysing laser, a stainless steel cell and an IR detector with appropriate signal processing system is shown in Fig. 1. The stainless steel cell used in this IR emission experiment has two orthogonal pairs of optical windows made of KCl.

* Tel.: +91-22-5505-148; fax: +91-22-5505-151.
E-mail address: pkc@apsara.barc.ernet.in (P.K. Chowdhury).

1010-6030/03/$ – see front matter
PII: S1010-6030(02)00349-0

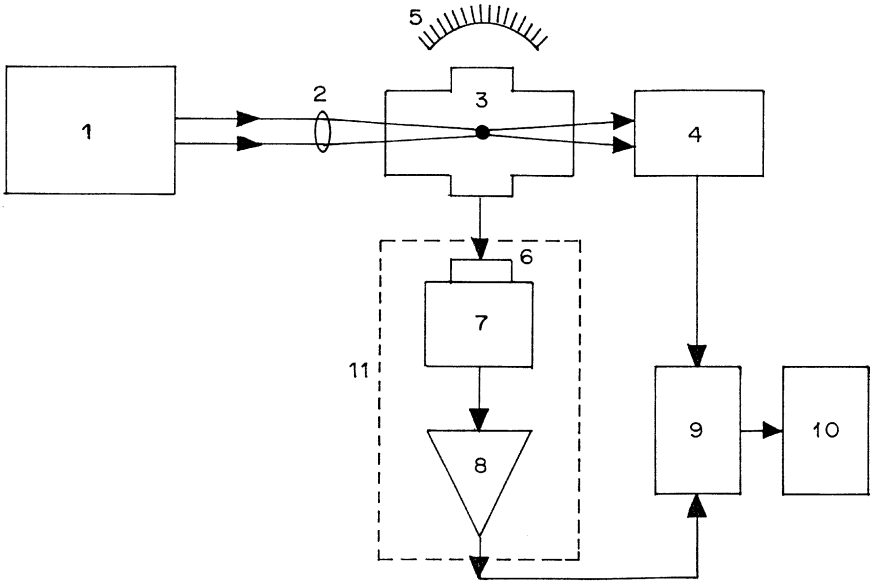

Fig. 1. A schematic diagram of the IRF apparatus: (1) CO_2 laser, (2) Ge and BaF_2 converging lens, (3) photolysis cell, (4) HgCdTe fast detector to trigger biomation, (5) concave mirror, (6) circular variable filter (OCLI), (7) In–Sb detector (77 K), (8) preamplifier, (9) biomation digitizer, (10) chart recorder and (11) Faraday cage.

Radiation from a pulsed TEA-CO_2 laser (Lambda Physik model EMG-201E) entered and exited through one pair of KCl windows. The laser pulse energy was measured by a pyroelectric detector (Gentec, model ED-200). The IR emission was collected at right angles to the laser beam by another pair of KCl windows. A 2 in. diameter *f*/2 gold coated concave mirror was placed behind one of the KCl window for enhancing better collection to the detector placed in front of the other window. The radiation after appropriate filtering with band-pass filters and cold gas cell was detected by a liquid N_2 cooled In–Sb detector (Judson Infrared Inc., J-10 D, photovoltaic type), equipped with a sapphire window and a matched preamplifier. The output signals from the preamplifier was fed to a biomation (Gould 4500) digital oscilloscope for digitization and averaging. The output of the averager was plotted using a *Y–T* chart recorder. The laser pulse picked up with a room temperature HgCdTe fast IR detector was used as a trigger for the transient digitizer. The overall time response of the system was about 1.2 μs, but the detector was found to be susceptible to radio frequency pick-up interference from the laser. Therefore, the detector assembly was shielded by a Faraday cage made of copper cylinder to minimize the electrical interference. The laser beam, being focused by a combination of a BaF_2 lens ($f = 200$ cm) and a Ge lens ($f = 10$ cm), was used for irradiating the propynal gas sample and a band-pass interference filter transmitting at 4.7 μm (FWHM 50 cm^{-1}) was used to isolate the proper wavelength region.

The IR emission spectrum was obtained by using a circular variable IR filter (CVF, OCLI 902) which was directly mounted on the detector for the maximum signal collection efficiency. The band-pass of the filter, in the experimental configuration, was about 50 cm^{-1}. The propynal was synthesized by the procedure of Sauer [9] and distilled before use. A conventional greaseless glass vacuum system was used for degassing the propynal by several freeze–pump–thaw cycles and for sample preparation. The reaction products were analyzed on a Fourier-transformed IR (FT-IR) spectrophotometer (Cygnus 100, Mattson) and a homemade gas chromatograph (GC). In GC analyses, CO was analyzed on a molecular sieve 5A column and thermal conductivity detector with helium as the carrier gas, whereas acetylene was separated on a silica gel column at room temperature and detected with a flame ionization detector.

3. Results and discussions

3.1. IR laser chemistry

IR spectroscopic analysis of propynal has been reported [10]. Propynal has a strong absorption band at 1697 cm^{-1} due to C–O stretch, a band at 2106 cm^{-1} due to C≡C stretch, two strong absorption bands at 2858 and 3326 cm^{-1} due to C–H stretch. It shows a very strong absorption band at 944 cm^{-1} due to C–C stretching mode which has an average absorption cross-section $\sigma = 6 \times 10^{-20}$ cm^2. On irradiation of 2 Torr propynal with a pulsed CO_2 laser at 10P(20), i.e. 944 cm^{-1}, in loosely focussed geometry with a fluence of 10–20 J/cm^2, the FT-IR absorption spectra were taken. Absorption feature appeared at 730 cm^{-1} is assigned to acetylene. The absorbance of the peak at 944 cm^{-1} decreases with the number of irradiating laser pulses. The decomposition

yield per pulse, α, is given by the following expression:

$$\alpha = \frac{\ln([\text{propynal}]_0/[\text{propynal}]_n)}{n} \quad (1)$$

where $[\text{propynal}]_0$ and $[\text{propynal}]_n$ are the propynal concentrations before and after irradiation with n pulses, respectively.

On GC analysis of 2 Torr propynal after 100 CO_2 laser pulses tuned at 10P(20) with a fluence of 15 J/cm^2, the product yield obtained was as follows: CO (100%), and C_2H_2 (99%). The amount of CO formed accounted for the total oxygenated products and that it satisfied the stoichiometric need, i.e. moles of CO = moles of C_2H_2. The overall mass balance between the yields of these products and propynal dissociated was within the experimental accuracy of ±2%. On repeating the irradiation in presence of NO or oxygen, the nature of the products as well as their mass balance remained unchanged. This fact suggests that the products are formed via non-radical dissociation channel of propynal induced by IR multiphoton excitation in the ground electronic state.

3.2. Time resolved IR emission

Upon excitation of 2 Torr propynal by the CO_2 laser operating near 943 cm^{-1}, very strong IR fluorescence was observed. The fluorescence spectrum taken at 3 μs by using the circular variable filter is shown in Fig. 2, showing two bands at 2800 and 2140 cm^{-1}. The broad emission band at 2140 cm^{-1} has been assigned to the vibrationally excited CO ($\nu = 1$), CO ($\nu > 1$) and the C≡C stretching mode of excited propynal. The broad emission at 2800 cm^{-1} with a shoulder at 3240 cm^{-1} has been assigned to the C–H stretching mode of propynal and excited acetylene products, respectively. The emission at 1700 cm^{-1} has been assigned to the ≻C=O stretch of propynal. The above assignments are confirmed by recording the spectrum using the cold gas filters with acetylene and propynal, respectively. With a CO gas filter, the longer wavenumber side of the 2140 cm^{-1} band disappears and the shorter wavenumber side corresponding to the C≡C stretching mode remains. Molecules excited in high vibrational levels can decay via IR emission, dissociation and quenching. The deactivation by IR emission is rather slow and has a decay time of about 0.1 s [11], but this process may be important at very low pressures. Propynal molecules excited below their threshold energy level for dissociation, are cooled down by this IR emission and collisional energy loss processes.

A typical time resolved fluorescence signal at 2140 cm^{-1} is shown in Fig. 3. This is characterized by a rapid fluorescence rise and a considerably slower decay which is single exponential to within experimental error. The rise-time of the signal is limited apparently by the band-width of the detection system. The rate constant, with the above limitation of the experimental response time, for the rising signal is found to be the same at 2140 and 2800 cm^{-1}, viz. 8×10^5 s^{-1}. Decay rates were determined from the IRF decay curves by fitting semilog plots of fluorescence intensity vs. time. These rates were measured as a function of propynal pressure over a range 0.3–3 Torr. The slope of the plots of the decay rates at 2140 cm^{-1} against propynal pressure (Fig. 4) gives a decay rate constant of 1540 ± 200 Torr^{-1} s^{-1}. This is assigned to the intermolecular V–V relaxation of CO ($\nu = 1$) by propynal's near resonant ν_3 vibrational mode (C≡C stretch) at 2106 cm^{-1} which is about 37 cm^{-1} lower than the CO vibrational quanta. The V–V relaxation rate constant of CO ($\nu = 1$) has been reported to be 819 Torr^{-1} s^{-1} by CF_3Br

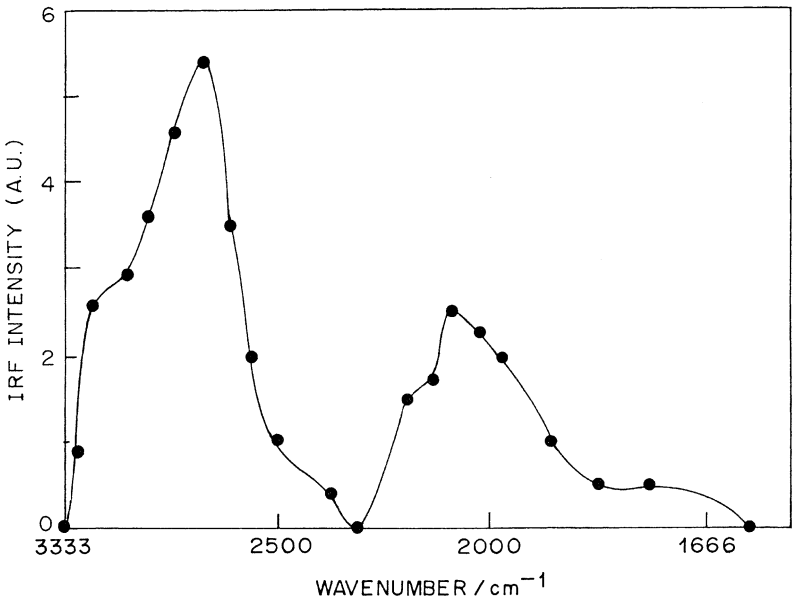

Fig. 2. IR fluorescence spectrum at 3 μs in the region of 3333–1600 cm^{-1} after CO_2 laser excitation of 2 Torr propynal.

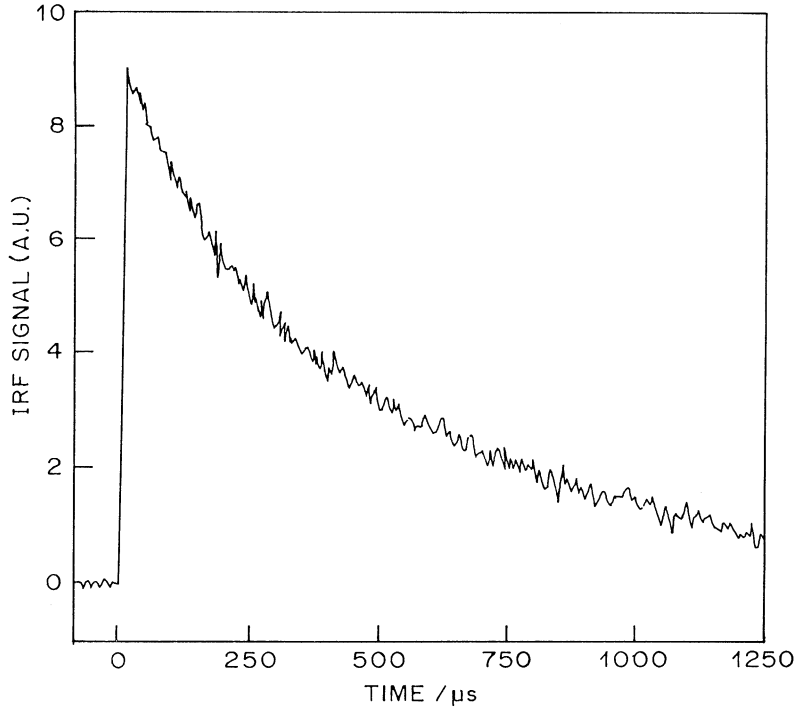

Fig. 3. IR fluorescence of the CO ($\nu \geq 1$) fragment at 2140 cm^{-1} after CO_2 laser excitation of 1.1 Torr propynal. The decay rate is governed by vibrational energy transfer to propynal.

[12] and 4700 $Torr^{-1}\,s^{-1}$ by CH_3CHO [13]. Although the vibrational relaxation rate with propynal has not been reported earlier, the rate constant of CO ($\nu = 1$) could presumably be higher than our measured value of 1540 $Torr^{-1}\,s^{-1}$. Due to large availability of product energy, it seems possible that some of the CO molecules are formed with higher vibrational excitation, i.e. $\nu > 1$, which is likely to decay by steps. The above decay rate constant, 1540 $Torr^{-1}\,s^{-1}$, may be considered as a lower limit. Recently we have observed [20] a V–V relaxation rate constant of CO ($\nu = 1$) with acrolein as 1240 $Torr^{-1}\,s^{-1}$. The IR emission bandshape was reproduced with an average vibrational excitation of CO with

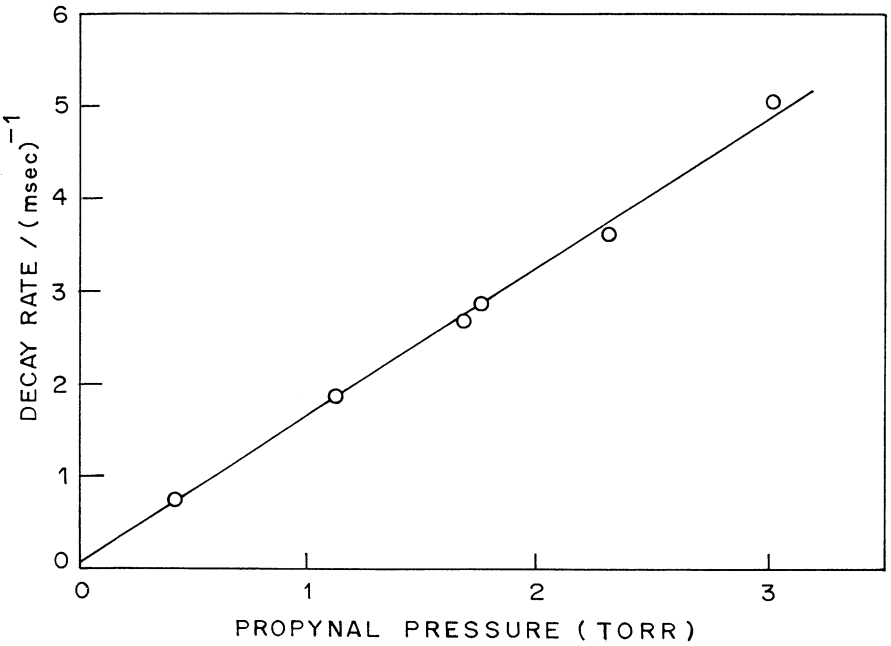

Fig. 4. Deactivation rate of CO ($\nu \geq 1$) IRF at 2140 cm^{-1} vs. propynal pressure. The slope obtained is 1540 ± 200 $Torr^{-1}\,s^{-1}$.

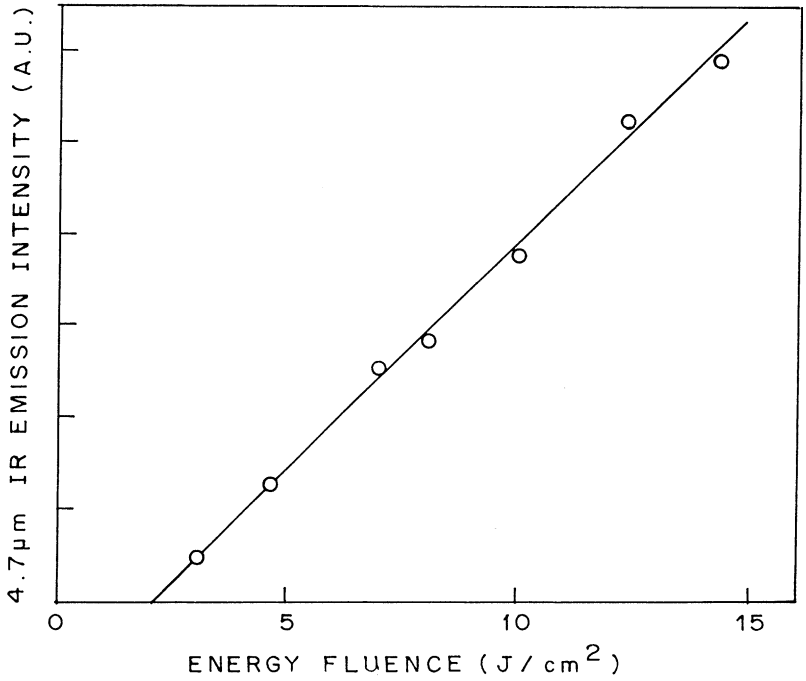

Fig. 5. The CO ($v \geq 1$) IR emission intensity vs. laser energy fluence ($J\,cm^{-2}$) at the 10P(20) CO_2 laser irradiation of 2 Torr propynal.

$v = 4$ [21]. However, such a detailed spectroscopic analysis of the emission spectra at 2140 cm^{-1} could not be performed here, due to the overlapping emission of propynal's near resonant ν_3 vibrational mode (C≡C stretch) at 2106 cm^{-1}.

In another study, the IRF intensity at 4.7 μm was monitored as a function of the CO_2 laser fluence: the result is shown in Fig. 5. The CO ($v = 1$) production appears to be linear in the fluence range studied, with a threshold fluence of about $2.1 \pm 0.2\,J\,cm^{-2}$ required for the initiation of IRMPD in propynal. When the experiment was repeated for the 2800 cm^{-1} IRF, a much lower threshold fluence of about $0.5 \pm 0.1\,J\,cm^{-2}$ was obtained. This appears to be the threshold fluence required for the excitation of propynal through quasi-continuum where energy randomization populates its ν_2 C–H stretching vibrational mode at 2800 cm^{-1}.

3.3. Dissociation mechanism of ground state vs. electronically excited propynal

The propynal UV spectrum shows a very weak absorption starting from 414 nm and extends towards shorter wavelength. The absorption spectrum becomes slightly stronger from 382 nm onwards. These absorption systems are assigned to the $n \rightarrow \pi^*$ transitions from the ground S_0 to the first triplet (T_1) and singlet (S_1), respectively. At 206 nm, it shows a strong and diffuse absorption band which has been assigned to the $\pi \rightarrow \pi^*$ transition [14]. In the gas phase photolysis of propynal with the (n, π^*) S_1 or T_1 excitation at 300–400 nm, Stafast et al. [7] found that the molecular CO and C_2H_2 are produced after the internal conversion to the ground state. Haas et al. [8] reported three dissociation channels in the molecular beam photofragmentation of propynal at 193 nm: first, the radical channel to form C_2H and HCO; second, the hydrogen atom channel involving aldehyde C–H bond fission; and finally, the molecular channel to form CO and C_2H_2. The fission energy of the aldehydic C–H bond has been determined by Willmott et al. [6] as 86.6 kcal/mol, indicating the absence of stabilization due to the acetynyl group. The above results suggest that there are three primary dissociation channels of propynal:

$$HC{\equiv}C\text{–}CHO \rightarrow C_2H_2 + CO, \quad \Delta H^\circ = 2\,kcal/mol \qquad (I)$$

$$HC{\equiv}C\text{–}CHO \rightarrow CH{\equiv}C + HCO, \quad \Delta H^\circ = 117\,kcal/mol \qquad (IIa)$$

$$CHO \rightarrow H + CO, \quad \Delta H^\circ = 16\,kcal/mol \qquad (IIb)$$

$$HC{\equiv}C\text{–}CHO \rightarrow HC{\equiv}C\text{–}CO + H, \quad \Delta H^\circ = 87\,kcal/mol \qquad (IIIa)$$

$$HC{\equiv}C\text{–}CO \rightarrow HC{\equiv}C + CO, \quad \Delta H^\circ = 46\,kcal/mol \qquad (IIIb)$$

The reaction enthalpies are estimated on the basis of group additivity methods [15]. Reaction (I) produces CO directly via synchronous C–C and C–H bond rupture, whereas reactions (II) and (III) produce CO as a secondary product via the dissociation of the formyl and HC≡C–CO radicals, respectively. The reported [8] mass spectrometric detection

of the product yields in the molecular beam photodissociation of propynal at 193 nm suggests that all three reaction channels (I, II and III) open up with almost equal probability.

In comparison with the UV photochemistry, our results clearly indicate that multiphoton vibrationally excited propynal dissociates via molecular mechanism (I). Formation of CO via (II and III) requires a minimum of 133 kcal/mol. In the current experiments, CO is produced with a significant vibrational excitation, in spite of an average propynal multiphoton excitation level of 75 kcal/mol (cf. Section 3.4). Further, in absence of any radical bearing C_3 product or any effect by radical quenchers, the reaction channel (II and III) is ruled out. With an exit barrier of 66 kcal/mol involved in the dissociation of propynal via (I), the nascent acetylene and CO molecules are expected to be formed in their vibrationally excited states.

3.4. Energy distribution and dissociation rates

By irradiation with the pulsed CO_2 laser tuned at the 10P(10) line, the dissociation yield of propynal, α, was found to decrease by addition of SF_6 to 0.5 Torr of propynal. Plot of α vs. SF_6 quencher pressure yielded a straight line as shown in Fig. 6. IR spectra of the post irradiated sample was taken to see if there is any depletion of the SF_6 concentration and any products formed from SF_6 dissociation. However, no SF_6 dissociation could be monitored. It has been found by us earlier [16] that the decrease in decomposition yield could be treated as a competition between collisional deactivation and unimolecular decomposition, i.e.

$$\alpha = \frac{\langle k \rangle}{\langle k \rangle + \omega\beta P}\alpha_0 \quad (2)$$

where values of the mean rate constant $\langle k \rangle$ for the unimolecular decomposition can be evaluated at different added buffer gas pressures, P, by using the deactivation efficiency β and the hard sphere collision frequency ω for SF_6. The deactivation efficiency (β) of SF_6 is considered as unity and $\omega = \sigma^2(8\pi RT/\mu)^{1/2}$. Adopting σ(propynal) = 4.8 Å and $\sigma(SF_6)$ = 4.2 Å, collisional frequency (ω) is calculated to be $9.0 \times 10^6\ s^{-1}\ Torr^{-1}$. (As $P \to 0$, $\alpha \to \alpha_0$.) The values of $\langle k \rangle$ are dependent on the mean internal energy content of the propynal molecules which decreases as the collision rate increases. This results in an exponential decrease of $\langle k \rangle$ with the SF_6 buffer gas pressure. The plot of ln(k) vs. SF_6 pressure is given in Fig. 7. Extrapolation of the plot to zero SF_6 pressure provides with the rate constant, $k_0 \sim (1.5 \pm 0.2) \times 10^7\ s^{-1}$, for the dissociation of propynal under collisionless conditions.

Rice–Ramsperger–Kassel–Marcus (RRKM) calculation of the rate of dissociation leads to an estimate of the internal energy of the propynal molecule. A frequency factor of $\log A\ (s^{-1}) = 14.4$, and an activation barrier of E_{act} = 68 kcal/mol have been reported for the unimolecular dissociation of propynal [17] which generates CO and acetylene as products. Unimolecular rate constants $k(E)$ are calculated using the conventional RRKM theory and the sum and density of states are calculated using Whitten–Rabinovitch approximations [18]. A rigid activated complex has been assumed for the concerted CO elimination from propynal.

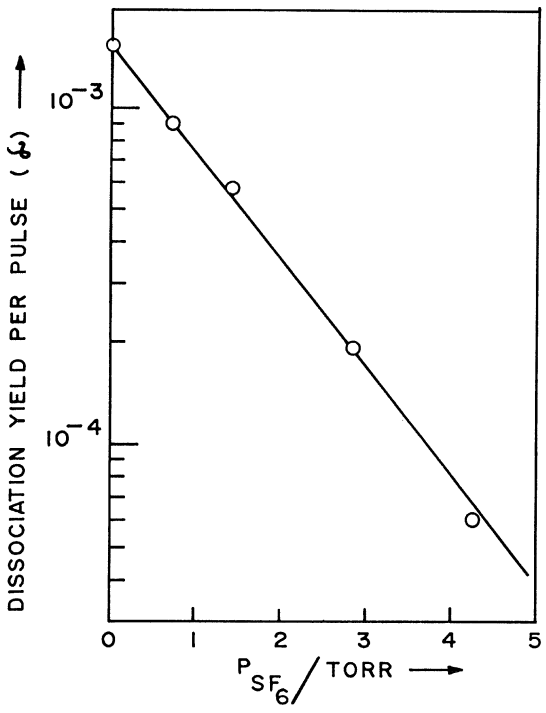

Fig. 6. Dissociation yield per pulse (α) of 0.5 Torr propynal at 10P(10) CO_2 laser irradiation as a function of added buffer gas pressure of SF_6.

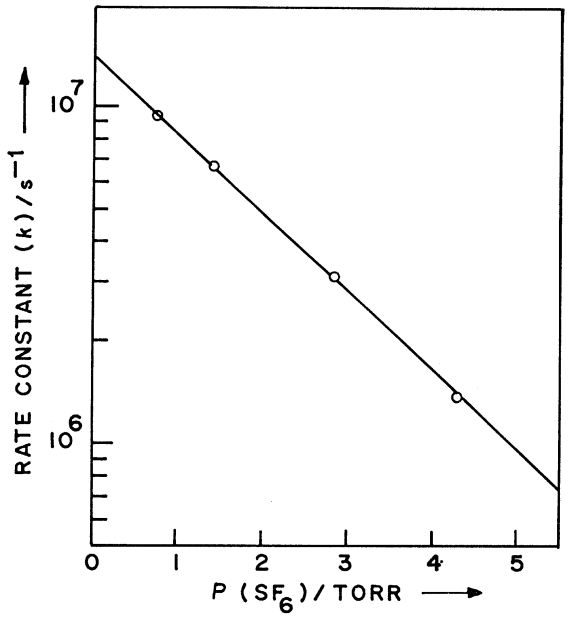

Fig. 7. Multiphoton dissociation rate constant (k) as a function of buffer gas pressure SF_6.

Table 1
Parameters used in RRKM calculations

Vibrational wavenumbers (cm^{-1})	
Propynal molecule (Ref. [10])	Activated complex
3326, 2858*, 2106, 1696, 1389*, 981*, 944, 650*, 614*, 261*, 205*, 193*	Same as propynal except those numbers with asterisks replaced by 1850, 1200, 700, 550, 510, 150, 140 and 130. 944 is dropped since it is considered as the reaction coordinate. $\log A\ (s^{-1}) = 14.4$, critical energy $= 68\,kcal\,mol^{-1}$, reaction path degeneracy $= 1$

The C–C stretching mode at $944\,cm^{-1}$ has become the reaction coordinate and other related vibrational frequencies are adjusted until the agreement reaches between the A factor and the corresponding values calculated from the predicted entropy of activation. The frequencies taken for the activated complex and other parameters used in the RRKM calculations are given in Table 1. In correspondence with the dissociation rate of $1.5 \times 10^7\,s^{-1}$, one obtains a mean excitation energy of propynal to be about 75 ± 4 kcal/mol.

In the dissociation of propynal, CO and acetylene will carry away most of the internal energy, because acetylene has a large number of low frequency vibrational modes. If statistical partitioning of the energy is assumed [19], the CO vibrational mode will have about 8.5% of the total energy released in products. As the total energy available for products ($E_{total} = nh\nu - \Delta H^\circ + 3RT$) is about 75 kcal/mol, an average vibrational energy associated with CO is nearly equivalent to a vibrational quantum.

RRKM theory is a statistical treatment, which calculates the rate of a system crossing a hypothetical transition state. In principle, it can predict nothing about the state distribution of the products. At the transition state the dissociation coordinate is normal to the dividing surface between the reactants and products. For the present case of propynal, as the H-atom transfers from the attached C=O group to the acetylenic group, the C–C bond linking the CO to the acetylene breaks. In other words, the dissociation coordinate is complex and depends on the position of H-atom and other atoms rather than merely on the C–C distance of the dissociating bond. If a nearly collinear C–C=O transition state configuration of the molecule at the moment of dissociation is assumed, the sudden C–C break would directly affect the vibrational excitation of the C=O fragment. The molecular fragments may be produced on the time scale of a vibrational period, which may yield a non-statistical energy distribution in the product CO, as found in our earlier observation [20,21] on the multiphoton dissociation of acrolein.

4. Conclusions

Multiphoton vibrationally excited propynal undergoes concerted dissociation generating CO and acetylene. The vibrationally excited nascent product CO is detected immediately following the CO_2 laser pulse by observing IR emission at 4.7 μm. The decay of the IR emission was studied as a function of propynal pressure. A vibrational–vibrational (V–V) relaxation rate constant of CO ($\nu \geq 1$) by propynal is found to be $1540 \pm 200\,Torr^{-1}\,s^{-1}$. The threshold fluence required for the IR multiphoton dissociation of propynal has been found to be $2.1\,J/cm^2$. Under collisionless condition, propynal dissociates with a rate constant of $(1.5 \pm 0.2) \times 10^7\,s^{-1}$. RRKM calculation with the above dissociation rate, suggests an average IR multiphoton excitation level of propynal to be $75 \pm 4\,kcal\,mol^{-1}$.

Acknowledgements

It is a great pleasure to acknowledge Dr. J.P. Mittal for valuable discussions and K.A. Rao for helping with the GC analysis. The author wishes to thank Dr. T. Mukherjee and Dr. A.V. Sapre for their keen interest in this work.

References

[1] E.K.C. Lee, R.S. Lewis, Adv. Photochem. (1980) 12.
[2] W.M. Jackson, H. Okabe, Adv. Photochem. (1986) 23.
[3] C.B. Moore, J.C. Weisshaar, Annu. Rev. Phys. Chem. 34 (1983) 525.
[4] D.J. Bamford, S.V. Filseth, M.F. Foltz, J.W. Hepburn, C.B. Moore, J. Chem. Phys. 84 (1986) 6519.
[5] M.C. Chung, M.F. Foltz, C.B. Moore, J. Chem. Phys. 87 (1987) 3855.
[6] P.R. Willmott, H. Bitto, J.R. Huber, Chem. Phys. 156 (1991) 177.
[7] H. Stafast, H. Bitto, J.R. Huber, J. Chem. Phys. 79 (1983) 3660.
[8] B.M. Haas, T.K. Minton, P. Felder, J.R. Huber, J. Phys. Chem. 95 (1991) 5149.
[9] J.C. Sauer, Org. Synth. Coll. 4 (1963) 813.
[10] J.C.D. Brand, J.H. Callomon, J.K.G. Watson, Disc. Faraday. Soc. 35 (1963) 175.
[11] L.J. Allamandola, A.G.G.M. Tielens, J.R. Barker, Astrophys. J. Suppl. Ser. 71 (1989) 733.
[12] E.T. Macke, H. Hellfeld, R.A. McFarlane, C.C. Davis, J. Chem. Phys. 69 (1978) 4564.
[13] J.C. Stephenson, E.R. Mosburg Jr., J. Chem. Phys. 60 (1974) 3562.
[14] J.K.G. Watson, Ph.D. Thesis, Glasgo, 1962.
[15] S.W. Benson, Thermochemical Kinetics, 2nd ed., Wiley, New York, 1976.
[16] P.K. Chowdhury, K.V.S. Rama Rao, J.P. Mittal, J. Phys. Chem. 90 (1986) 2877.
[17] H. Stafast, R. Pfister, J.R. Huber, J. Chem. Phys. 89 (1985) 5074.
[18] P.J. Robinson, K.A. Holbrook, Unimolecular Reactions, Wiley/Interscience, New York, 1972.
[19] D.B. Galloway, T. Glenewinkel-Meyer, J.A. Bartz, L.J. Huey, F.F. Crim, J. Chem. Phys. 100 (1994) 1946.
[20] P.K. Chowdhury, K.V.S. Rama Rao, J.P. Mittal, Chem. Phys. Lett. 218 (1994) 60.
[21] P.K. Chowdhury, Chem. Phys. 260 (2000) 151.